

Downregulation of AMP-activated protein kinase by Cidea-mediated ubiquitination and degradation in brown adipose tissue

Jingzong Qi^{1,3}, Jingyi Gong^{1,3},
Tongjin Zhao^{1,3}, Jie Zhao¹, Penny Lam²,
Jing Ye¹, John Zhong Li², Jiawei Wu¹,
Hai-Meng Zhou^{1,*} and Peng Li^{1,*}

¹Protein Science Laboratory of Ministry of Education, Department of Biological Sciences and Biotechnology, Tsinghua University, Beijing, China and ²Department of Biology, Hong Kong University of Science and Technology, Clearwater Bay, Kowloon, Hong Kong

We previously showed that *Cidea*^{-/-} mice are resistant to diet-induced obesity through the upregulation of energy expenditure. The AMP-activated protein kinase (AMPK), consisting of catalytic α subunit and regulatory subunits β and γ , has a pivotal function in energy homeostasis. We show here that AMPK protein levels and enzymatic activity were significantly increased in the brown adipose tissue of *Cidea*^{-/-} mice. We also found that *Cidea* is colocalized with AMPK in the endoplasmic reticulum and forms a complex with AMPK *in vivo* through specific interaction with the β subunit of AMPK, but not with the α or γ subunit. When co-expressed with *Cidea*, the stability of AMPK- β subunit was dramatically reduced due to increased ubiquitination-mediated degradation, which depends on a physical interaction between *Cidea* and AMPK. Furthermore, AMPK stability and enzymatic activity were increased in *Cidea*^{-/-} adipocytes differentiated from mouse embryonic fibroblasts or preadipocytes. Our data strongly suggest that AMPK can be regulated by *Cidea*-mediated ubiquitin-dependent proteasome degradation, and provide a molecular explanation for the increased energy expenditure and lean phenotype in *Cidea*-null mice.

The EMBO Journal (2008) 27, 1537–1548. doi:10.1038/emboj.2008.92; Published online 15 May 2008

Subject Categories: signal transduction; proteins

Keywords: AMPK; brown adipose tissue; *Cidea*; protein degradation; ubiquitination

Introduction

Impaired energy homeostasis often results in obesity and type II diabetes (Spiegelman and Flier, 2001). Brown adipose tissue (BAT) has a unique function in energy expenditure by converting excessive energy to heat and in maintaining body

*Corresponding author. H-M Zhou or P Li, Department of Biological Sciences and Biotechnology, Tsinghua University, Beijing 100084, China. Tel.: +86 10 62797121; Fax: +86 10 62797123; E-mail: li-peng@mail.tsinghua.edu.cn

³These authors contributed equally to this work

Received: 11 October 2007; accepted: 11 April 2008; published online: 15 May 2008

temperature when animals are exposed to cold. *Cidea*, belonging to the CIDE family that include *Cideb* and *Cidec/Fsp27*, was originally identified by its sequence homology with the N-terminal region of DNA fragmentation factor (DFF) (Inohara *et al*, 1998). Previously, we found that *Cidea* is expressed at very high levels in BAT (Zhou *et al*, 2003). Using *Cidea*-null mice as a model system, we demonstrated that *Cidea*-null mice have increased energy expenditure, reduced levels of plasma triacylglycerides and free fatty acids, and are resistant to high fat diet-induced obesity and diabetes (Zhou *et al*, 2003). These data suggest that *Cidea* has an important function in regulating energy homeostasis. Recently, *Cidea* was implicated in human obesity by regulating human adipocyte lipolysis (Nordstrom *et al*, 2005) and a V115F polymorphism in human *Cidea* was found to be closely associated with obesity (Dahlman *et al*, 2005), underscoring the importance of *Cidea* in obesity development among humans. The expression levels of *Cidea* in human adipocytes were inversely correlated with the basal metabolic rate (Gummesson *et al*, 2007). In addition, when mice were fed with a high-calorie diet, *Cidea* mRNA is dramatically upregulated in the liver (Baur *et al*, 2006). All these data suggest that *Cidea* could negatively regulate energy expenditure in BAT.

The AMP-activated protein kinase (AMPK) is an evolutionarily conserved metabolic sensor and has a pivotal function in maintaining energy homeostasis. AMPK exists as a heterotrimeric complex consisting of catalytic α subunit and regulatory subunits β and γ (Kahn *et al*, 2005; Hardie *et al*, 2006). The β subunit exerts an effect as a scaffold protein to provide docking sites for both α and γ subunits at its C terminus. AMPK activity can be influenced by their subcellular localization (Salt *et al*, 1998; Warden *et al*, 2001). The γ subunit of AMPK contains four cystathionine beta-synthase repeats that bind to AMP or ATP in a mutually exclusive manner (Scott *et al*, 2004). Crystal structure of ATP- and AMP-bound forms of a core α , β and γ adenylate-binding complex suggests that ATP and AMP bind competitively to a single site in the γ subunit (Townley and Shapiro, 2007; Xiao *et al*, 2007). AMPK is activated by rising AMP concentrations coupled with falling ATP concentrations. Activation of AMPK is also dependent on the phosphorylation of α subunit at residue Thr-172 by upstream kinases such as LKB1 (Hawley *et al*, 2003; Woods *et al*, 2003) and CaMKK (Hawley *et al*, 2005; Hurley *et al*, 2005; Woods *et al*, 2005). AMPK has also been shown to mediate metabolic regulation of several hormonal pathways including the ones for leptin (Minokoshi *et al*, 2002), adiponectin (Yamauchi *et al*, 2002), resistin (Banerjee *et al*, 2004) and α -adrenergic hormones (Kishi *et al*, 2000; Minokoshi *et al*, 2002). Biguanides such as metformin and thiazolidinediones that are commonly used as antidiabetic drugs can also induce AMPK activity (Daval *et al*, 2005; Huypens *et al*, 2005) in muscle and adipocytes. Being able to respond to diverse hormonal

signals, AMPK serves as a signal integrator in peripheral tissues, as well as in the hypothalamus for the control of whole-body energy homeostasis (Long and Zierath, 2006; Xue and Kahn, 2006).

Active AMPK achieves its regulatory effects by either rapid phosphorylation of various metabolic enzymes or through long-term regulation of target gene expression. It has a crucial function in regulating energy homeostasis in adipose tissue by controlling fatty acid oxidation, glucose uptake and lipolysis (Daval *et al*, 2006). One well-characterized AMPK target in adipose tissue is acetyl CoA carboxylase-1/2 (ACC1/2). Phosphorylation by AMPK leads to reduced ACC activity, resulting in lower levels of malonyl-CoA production but increased fatty acid oxidation (Steinberg *et al*, 2006). Elevated AMPK activity is believed to account for the lean and insulin-sensitive phenotype in *SCD1*-null mice (Dobrzyn *et al*, 2004). Recently, several novel downstream effectors of AMPK have been identified, suggesting that AMPK controls an increasingly broad range of cellular processes including cellular structure and cell volume (Lee *et al*, 2007). In addition, several proteins including TSC2 (Inoki *et al*, 2003), FNIP1 (Baba *et al*, 2006) and CFTR (Hallows *et al*, 2000) have been reported to associate with AMPK. However,

little is known as to how the AMPK enzyme complex is regulated. In particular, although relatively fast turnover of AMPK- α was observed when overexpressed in COS-7 cells (Crute *et al*, 1998), it remains unclear if endogenous AMPK activity can be controlled at the level of protein stability. In this study, we show that Cidea is an AMPK-interacting protein and is an important regulator for AMPK stability. We have thus unravelled a molecular mechanism for AMPK stability that is mediated by Cidea and provided an explanation as to why deficiency of *Cidea* results in lean phenotypes.

Results

AMPK protein levels and its enzymatic activity are increased in BAT of *Cidea*^{-/-} mice

In the course of searching for a molecular explanation for the lean phenotype of *Cidea*-null mice, we analysed the expression levels of AMPK and observed that the protein levels of AMPK- α , - β and - γ subunits were all significantly increased in BAT of *Cidea*-null mice (approximately 50% higher than those in wild-type mice; Figure 1A), whereas no difference in mRNA levels was detected (data not shown). The amount of phosphorylated AMPK- α , detected by a phospho-specific

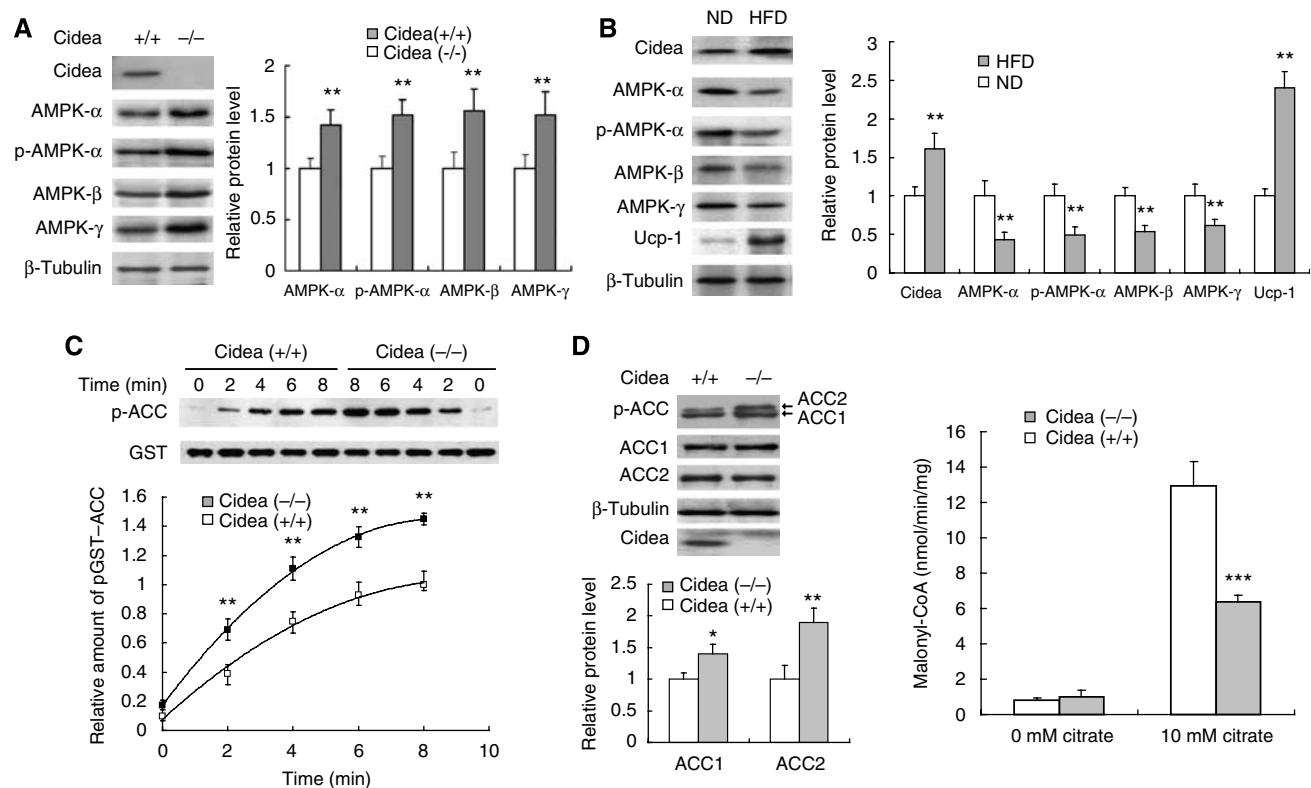


Figure 1 Increased AMPK levels and enhanced AMPK activity in BAT of *Cidea*^{-/-} mice. (A) Increased levels of AMPK- α , - β , - γ and phospho-AMPK- α in BAT of *Cidea*^{-/-} mice. BAT was collected from 3-month-old wild-type and *Cidea*^{-/-} male mice. β -Tubulin was served as a loading control. Similar experiments were carried out five times and the intensity of individual band in each western blot was quantified by TOTAL-LAB software (Nonlinear Dynamics, UK) and used for statistical analysis. The relative protein level in wild-type mice was designated as 1.0. ** P < 0.01. Similar quantitative and statistical analyses were conducted for all western blots shown in following figures. (B) BAT of high-fat diet (HFD)-treated mice had increased Cidea level and decreased AMPK levels compared with that of normal diet (ND)-fed animals. Similar experiments were conducted five times from five pairs of mice. The relative protein level of Cidea, Ucp1 and AMPK in mice fed with ND was designated as 1.0. (C) BAT of *Cidea*^{-/-} mice showed enhanced AMPK activity. The upper panel was the time course of AMPK activity in BAT of wild-type and *Cidea*^{-/-} mice. The lower panel was the quantitative analysis of the phospho-ACC western blot bands from four independent experiments. The relative intensity of phospho-GST-ACC in wild-type mice at 8 min was designated as 1.0. (D) BAT of *Cidea*^{-/-} mice showed increased endogenous ACC phosphorylation (left panel) and decreased ACC enzymatic activity (right panel). Four independent experiments were conducted using four pairs of mice (* P < 0.05, ** P < 0.01, *** P < 0.001).

antibody against phosphorylated T172, was also increased in BAT of *Cidea*-null mice (Figure 1A). Levels of AMPK in other tissues such as liver, white adipose tissue (WAT) or skeletal muscle were unchanged (data not shown), indicating that the increase in AMPK protein levels occurs specifically in the BAT of *Cidea*-null mice. This prompted us to wonder whether high-fat diet (HFD) could elevate *Cidea* protein levels in wild-type mice, and if so, what would occur to the protein levels of AMPK in these mice. When animals were fed with HFD for 8 weeks, their body weight was significantly increased compared with that of mice fed with normal diet (ND; Supplementary Figure 1). Levels of *Cidea* protein were approximately 50% higher ($P < 0.01$) in BAT of HFD-fed mice than that of ND-fed mice (Figure 1B). Levels of *Ucp1* were also increased in the BAT of HFD-fed mice. In contrast, levels of AMPK- α , - β and - γ subunits and phospho-AMPK- α were all significantly decreased ($P < 0.01$; Figure 1B). These data demonstrate that levels of AMPK are inversely correlated with the levels of *Cidea* in BAT.

To examine the consequence of increased AMPK protein levels, we established a convenient and non-radioactive AMPK assay (see Materials and methods). As judged by its sensitivity to AMP and to AICAR treatment, our new assay is as sensitive as the previously established SAMS peptide phosphorylation assay (Supplementary Figure 2A and B). Using this assay, we measured the endogenous AMPK activity in the BAT of *Cidea*^{-/-} mice *in vitro*, and observed that AMPK activity in *Cidea*^{-/-} BAT was approximately 50% higher compared with that of wild-type mice at various durations of reaction (Figure 1C), displaying a good correlation between the increase in enzymatic activity and the increase in AMPK protein levels. The increased AMPK activity is not due to elevated AMP level or decreased ATP level as the AMP/ATP ratio was similar in BAT of wild-type and *Cidea*-null mice (Supplementary Figure 2C). The K_m for ACC and ATP as assessed by kinetic analysis was similar between AMPK from wild-type and *Cidea*^{-/-} BAT (Supplementary Figure 2D and E), confirming that the increased AMPK activity in *Cidea*^{-/-} mice was not due to enhanced intrinsic catalytic activity of AMPK but is a direct consequence of increased AMPK protein levels. The AMPK activities in liver, kidney and WAT were similar between wild-type and *Cidea*^{-/-} mice (Supplementary Figure 2F), which is consistent with a lack of *Cidea* expression in these tissues. To further confirm that AMPK activity is increased in the BAT of *Cidea*-null mice, we checked levels of phospho-ACC, an AMPK target, and observed increased levels of phosphorylated ACC1 (40% higher) and ACC2 (100% higher) in the BAT of *Cidea*^{-/-} mice (Figure 1D, left panel). The increased levels of phospho-ACCs were not due to an increase in the protein levels of ACC1 or ACC2, as levels of both proteins were similar between wild-type and *Cidea*^{-/-} mice. ACC activity was approximately 50% lower in the BAT of *Cidea*^{-/-} mice ($P < 0.001$), consistent with increased ACC phosphorylation in *Cidea*^{-/-} mice (Figure 1D, right panel). These data strongly indicate that levels of AMPK protein and its enzymatic activity are significantly and specifically increased in the absence of *Cidea*.

Colocalization and interaction between *Cidea* and AMPK- β

To investigate how *Cidea* might regulate AMPK protein levels, we first checked the subcellular localization of *Cidea* and

AMPK in the BAT by biochemical fractionation of various organelles. Interestingly, we observed that majority of *Cidea* protein was detected in endoplasmic reticulum (ER) and Golgi-enriched fractions but not in nuclei or mitochondrial-enriched fractions (Figure 2A). Significant amount of AMPK- β and - γ was also detected in ER-enriched fraction (Figure 2A), overlapping with *Cidea*. Lower amount of AMPK- β and - γ proteins was detected in the cytosolic fraction but not in nuclei or mitochondrial-enriched fractions. The purity of mitochondrial- and ER-enriched fractions was checked by western blot analysis using antibodies against COXIV (a mitochondria-specific protein) and PDI (an ER-specific protein), respectively. Although ER and Golgi fractions appeared to contain some mitochondria as COXIV was detected in these fractions, *Cidea* and AMPK are ER specific as no *Cidea* or AMPK was detected in the mitochondrial-enriched fraction. The contamination of mitochondria in ER- and Golgi-enriched fractions was probably due to the large amount and high heterogeneity of mitochondria in BAT.

To further confirm the subcellular localization of *Cidea* and AMPK, we co-expressed *Cidea* and AMPK- β individually with ER-specific protein GFP-Cb5 in COS-7 cells and carried out immunofluorescent staining (Figure 2B). When co-expressed with GFP-Cb5, *Cidea* showed a granular staining pattern with strong overlapping with GFP-Cb5-positive ER network. Surprisingly, *Cidea* was not colocalized with the mitochondrial-specific marker Mitotracker. When overexpressed individually, AMPK- β was evenly distributed in the cell (including cytoplasm and nucleus), and did not show any specific overlapping with endogenous Calnexin-positive ER network, suggesting that AMPK- β is not localized to ER in the absence of *Cidea*. When *Cidea* and AMPK- β were overexpressed, *Cidea* still showed granular pattern, but overlapped with Calnexin ER network. However, when co-expressed with *Cidea*, the subcellular distribution of AMPK- β was changed from a diffused pattern to a punctate and granular structure, overlapping with *Cidea*. These data suggest that AMPK- β and *Cidea* are colocalized in the ER and the localization of AMPK- β is dependent on *Cidea* (Figure 2B). In contrast, AMPK- α and - γ proteins were not colocalized with *Cidea* when they were co-expressed in COS-7 cells (data not shown).

Next, we tested for a possible physical interaction between *Cidea* and AMPK by co-immunoprecipitation assay. We pulled down AMPK complex by using antibodies against AMPK- α , - β and - γ , respectively, followed by detection of *Cidea* in the immunoprecipitates. As a positive control, we first showed that the three subunits of AMPK form a tight complex (Figure 2C). As shown in Figure 2C, *Cidea* was readily detected in immunoprecipitates from antibodies against α , β and γ subunits of AMPK. The presence of *Cidea* in the AMPK complex was not due to nonspecific binding of *Cidea* as it can only be precipitated by *Cidea* antibody but not by control serum (Figure 2C, right panel). Importantly, when antibodies against *Cidea* were used for immunoprecipitation, AMPK complex was detected in wild-type mice but not in *Cidea*-null mice (Figure 2C). Formation of *Cidea*-AMPK complex was further evaluated by biochemical fractionation of protein extracts from mouse BAT tissue. *Cidea* protein was detected in two major fractions: fractions 4–8 and 17–20 (Figure 2D). Judging from the molecular weights (approximately 40–60 kDa) in fractions 17–20, it is likely that the detected *Cidea* represents its dimeric form as

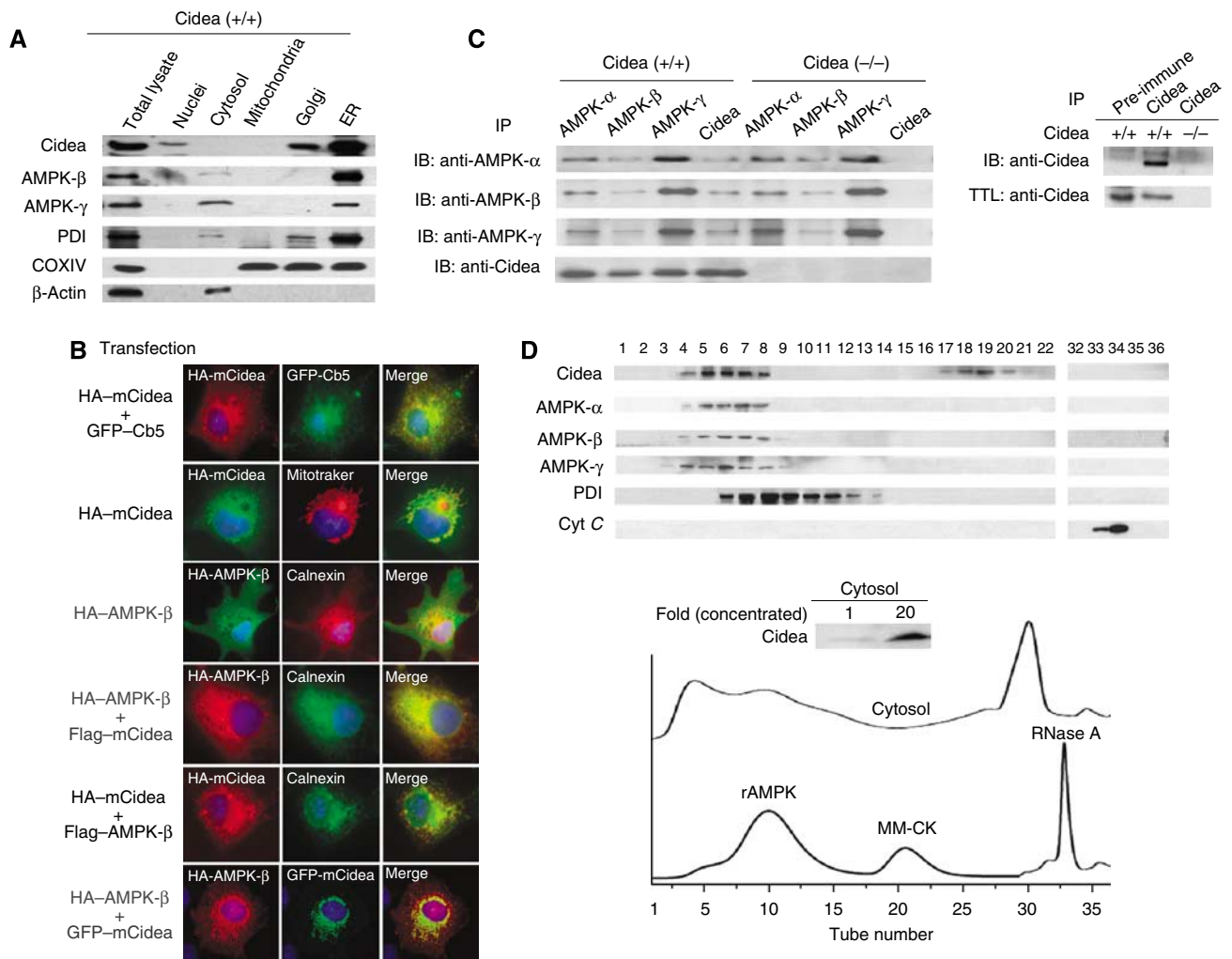


Figure 2 Cidea and AMPK are localized to ER and form a complex *in vivo*. **(A)** Cidea and AMPK are present in ER-enriched fraction. Protein disulphide isomerase (PDI), β -actin and COXIV were used as specific markers for ER, cytosol and mitochondria, respectively. **(B)** Cidea is localized to ER, and AMPK- β is colocalized with Cidea when co-expressed. HA-tagged mouse Cidea (HA-mCidea), HA-AMPK- β and endogenous Calnexin were visualized by immunofluorescence. Fields shown (magnification, $\times 600$) were visualized under fluorescence microscope at appropriate wavelengths for GFP (green), rhodamine (red) and Hoechst (blue), and the images were overlaid (merge, yellow). Plasmid DNAs used for transfection and immunostaining (transfection) were listed on the left side of each fluorescent staining image. **(C)** Cidea interacts with AMPK *in vivo*. Left panel, IP: immunoprecipitation using antibodies against AMPK- α , - β , - γ or Cidea in the immunoprecipitated products. Right panel, immunoprecipitation of Cidea by antibody against Cidea but not pre-immune serum. TTL: total tissue lysate. **(D)** Co-fractionation of Cidea and AMPK in cytosolic fraction of BAT. Bacterially expressed rat AMPK (rAMPK) complex (130 kDa), recombinant muscle-type creatine kinase (MM-CK; 86 kDa) and RNase A (14 kDa) were used as loading controls for gel filtration analysis. PDI (55 kDa) and cytochrome C (cyt C; 13 kDa) were used as controls for western blot analysis (insert of lower panel). Numbers on western blot correspond to the eluted fraction numbers from gel filtration chromatography.

we previously showed that CIDE family proteins can form dimers (Chen *et al*, 2000). Importantly, AMPK- α , - β and - γ were all detected in fractions 4–8, overlapping with the elution profile of Cidea (Figure 2D). Taken together, our data obtained from co-immunoprecipitation and biochemical fractionation analyses strongly indicate that Cidea and AMPK form a complex in the BAT.

We then asked which specific subunit(s) of AMPK directly interacts with Cidea by transfecting them in different combinations into 293T cells. AMPK- β , but not α and γ subunits, was co-precipitated with Cidea (Figure 3A). Reciprocally, when Cidea was immunoprecipitated with anti-Cidea antibody, AMPK- β but not AMPK- α or - γ was co-precipitated (Supplementary Figure 3). These data indicate that Cidea interacts specifically with AMPK- β . To delineate the region of

Cidea responsible for interaction with AMPK- β , we generated HA-tagged Cidea truncations containing the N-terminal domain (Cidea-N) or the C-terminal domain (Cidea-C), and co-expressed these mutants with FLAG-tagged AMPK- β . AMPK- β was co-precipitated with Cidea-C but not with Cidea-N (Figure 3B), indicating that the C-terminal region of Cidea is responsible for mediating its interaction with AMPK- β . To identify the region on AMPK- β responsible for interaction with Cidea, we generated a series of FLAG-tagged AMPK- β truncation constructs (listed in Figure 3C and D). Full-length AMPK- β and truncated AMPK- β proteins D2 (aa 68–270) and D4 (aa 187–270) containing C-terminal regions, co-precipitated Cidea (Figure 3C), indicating that the C-terminal portion of AMPK- β is necessary and sufficient to mediate the interaction with Cidea. Whereas AMPK- β (1–185) did not interact

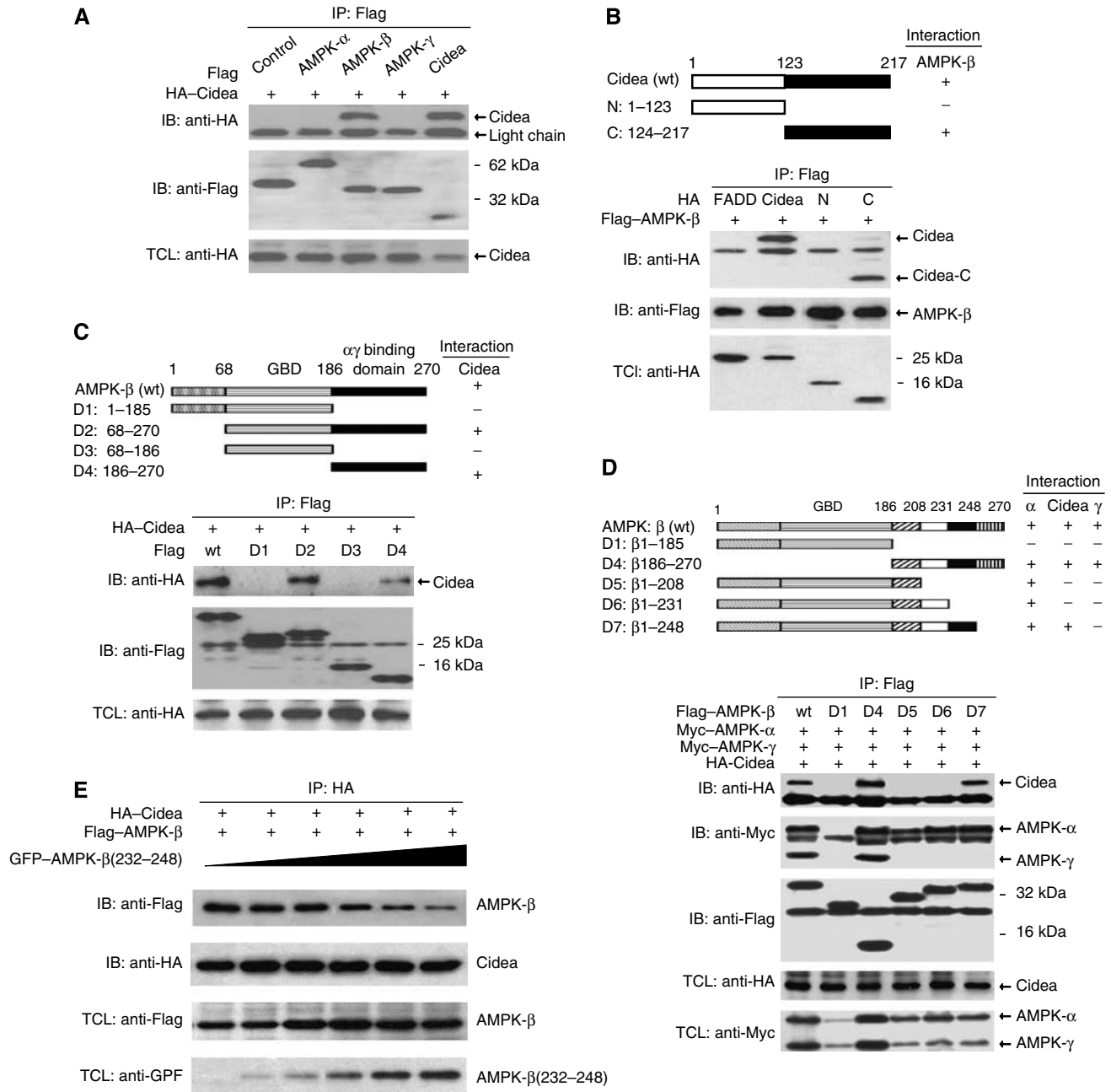


Figure 3 Specific interaction between Cidea and AMPK- β . (A) Cidea interacts with AMPK- β but not - α and - γ . HA-Cidea was co-transfected with Flag-AMPK- α , - β or - γ into HEK 293T cells. AMPK- α , - β , - γ or Cidea were immunoprecipitated (IP) by antibody against Flag. Immunoprecipitated products were detected by immunoblotting (IB) against HA and flag antibodies. HA-Cidea was used as a positive control, whereas Flag-JNK1 as a negative control. TCL, total cell lysate. (B) Mapping of the interface on Cidea that mediates the interaction between Cidea and AMPK- β . The upper panel shows a schematic diagram depicting different Cidea truncations. Flag-AMPK- β was co-transfected with HA-tagged full-length Cidea or its truncations (N and C). AMPK- β was immunoprecipitated (IP) using antibody against Flag and the co-precipitated products were detected by immunoblotting (IB) using antibody against HA. Fas-associated protein with death domain (FADD) was used as a negative control. (C, D) Identification of regions of AMPK- β crucial for mediating interactions with Cidea, AMPK- α and - γ . Schematic diagram (upper panels) depicted different AMPK- β truncations. Flag-AMPK- β deletions and HA-tagged full-length Cidea were co-transfected. Immunoprecipitation (IP) was carried out using antibody against Flag and the co-immunoprecipitated products were detected by immunoblotting (IB) using antibody against HA, Flag or Myc. (E) Truncated AMPK- β containing aa 232-248 blocked the interaction between Cidea and AMPK- β . Increasing amounts of GFP-AMPK- β (232-248) were co-transfected with HA-Cidea and Flag-AMPK- β . HA-Cidea was immunoprecipitated (IP) and their co-precipitated products were detected by immunoblotting (IB) using antibodies against HA or Flag. TCL, total cell lysate.

with AMPK- α , AMPK- β (1-208) could specifically co-immunoprecipitate AMPK- α (Figure 3D), suggesting that aa 186-208 are required to mediate the interaction with the α subunit. As AMPK- β (1-248) but not AMPK- β (1-231) showed

strong interaction with Cidea, the 17 amino-acid residues from aa 232 to 248 are important in mediating its interaction with Cidea. AMPK- β (186-270) showed interactions with the α , and γ subunits, as well as Cidea. These results indicate that

amino-acid residues at the extreme C-terminal of AMPK- β (249–270) is responsible for the interaction between AMPK- β and - γ subunits, consistent with a previous report (Iseli *et al*, 2005). When increasing amounts of AMPK- β deletion constructs that all include aa 232–248 were co-transfected with AMPK- β and Cidea, full-length AMPK- β detected in Cidea immunoprecipitates was gradually decreased, further confirming that the fragment of aa 232–248 in AMPK mediates the interaction with Cidea (Figure 3E). Our data have thus demonstrated that distinct and non-overlapping regions in the C-terminal portion of AMPK- β take part in interaction with AMPK- α , - γ and Cidea.

Cidea promotes AMPK- β degradation

The direct interaction between Cidea and AMPK- β , as well as the elevated AMPK protein levels in *Cidea*-null mice, all pointed to the possibility that Cidea may somehow regulate AMPK protein stability. We then examined the rate of AMPK- β degradation in the presence of cycloheximide (CHX), a protein synthesis inhibitor. In the presence of a non-interacting control protein FADD (Fas-associated protein with death domain), AMPK- β appears relatively stable, with more than 70% of the cellular AMPK- β remaining after 2 h of CHX treatment (Figure 4A). However, AMPK- β protein levels decreased rapidly when it was co-expressed with Cidea in the presence of CHX, with its half-life being less than 1 h (Figure 4A). In the presence of increasing amounts of Cidea, levels of AMPK- β protein were decreased in a dose-dependent manner (Figure 4B). These data indicate that Cidea can promote AMPK- β degradation when co-expressed. Enhanced AMPK- β degradation was also observed when it was co-expressed with the C-terminal but not the N-terminal domain of Cidea (Supplementary Figure 4A and B), suggesting that the C-terminal domain of Cidea, which mediates its interaction with AMPK- β , is sufficient to promote AMPK degradation. Cidea-mediated AMPK- β degradation appears to be also dependent on the interaction interface (aa 232–248) on AMPK- β , as the truncated form AMPK- β (1–231) that lacks the region for Cidea-AMPK- β interaction, is stable when co-expressed with Cidea (Figure 4C and Supplementary Figure 4B). Consistently, AMPK- β (1–248), including the segment of aa 232–248, undergoes rapid degradation when co-expressed with Cidea (Figure 4C and Supplementary Figure 4B). When co-expressed with AMPK- β and Cidea, GFP-AMPK β (232–248) can attenuate AMPK- β degradation by competitively binding to Cidea, further confirming that AMPK- β degradation is dependent on its interaction interface (aa 232–248) against Cidea (Figure 4D). These data suggest that Cidea can accelerate AMPK degradation and that their physical interaction is needed for this effect.

We then evaluated if the Cidea-enhanced degradation of AMPK- β depends on the ubiquitination-mediated proteosomal pathway. We found that MG132, a specific inhibitor of proteasome-mediated protein degradation, was able to block AMPK- β degradation, whereas NH₄Cl, a general lysosomal protease inhibitor, did not have such an effect (Figure 4E). We co-expressed AMPK- β , Cidea and Myc-tagged ubiquitin, followed by assays for ubiquitinated AMPK. In the presence of MG132, AMPK- β was weakly ubiquitinated in the absence of Cidea; Cidea alone was strongly ubiquitinated as previously reported (Chan *et al*, 2007) (Figure 4F). However, AMPK- β

ubiquitination was significantly increased when co-expressed with Cidea, in the presence of MG132. Increasing levels of AMPK- β ubiquitination were seen when increasing amounts of Cidea were expressed (Figure 4F). Furthermore, co-expression of increasing amounts of GFP-AMPK- β (232–248), which only contains the Cidea-binding domain and is able to compete against the interaction between full-length AMPK and Cidea, gradually attenuated the ubiquitination of AMPK- β (Figure 4F). Unlike AMPK- β , both AMPK- α and - γ are relatively unstable when expressed alone, but their rate of degradation was not accelerated when co-expressed with Cidea (Supplementary Figure 5), indicating that the role of Cidea in mediating AMPK- β degradation appears to be specific.

As we observed that AMPK levels are higher in the *Cidea*-null mice and that Cidea can enhance AMPK- β degradation, we carried out additional experiments to further evaluate if co-expression of the AMPK trimeric complex with Cidea could lead to accelerated degradation of the complex and decreased AMPK activity in 293T cells. When co-expressed as a trimeric complex in the absence of Cidea, all three subunits of AMPK were more stable compared with singly expressed ones as little protein degradation was observed for all three subunits over 2 h of CHX treatment (Figure 5A). In the presence of Cidea, protein levels of all three subunits were decreased dramatically, with only 60% of protein remaining after 2 h of CHX treatment (Figure 5A). The stability of AMPK complex was also dependent on the amount of Cidea as increased amount of Cidea accelerated their degradation (Figure 5B). Consistent with the decreased AMPK protein levels, AMPK activity was reduced when it was co-expressed with Cidea (Supplementary Figure 6A and B). The stability of AMPK complex was decreased when co-expressed with Cidea-C (binding to AMPK- β), but not Cidea-N (defective in binding to AMPK) (Figure 5C), confirming that the reduced AMPK complex stability is a consequence of its interaction with Cidea. Consistent with decreased AMPK protein levels, AMPK activity was also reduced in the presence of Cidea-C but not Cidea-N (Supplementary Figure 6C and D). These data suggest that Cidea can control the stability of AMPK complex through interacting with and targeting the β subunit for ubiquitination-dependent proteosomal degradation.

Increased AMPK stability and activity in *Cidea*^{-/-} adipocytes

To further evaluate the physiological role of Cidea proteins in the control of AMPK stability, we isolated mouse embryonic fibroblasts (MEFs) from wild-type and *Cidea*^{-/-} mice and induced them to differentiate to adipocytes *in vitro* under a specific condition as previously described (Ross *et al*, 1992) with the presence of triiodothyronine (T3) in the differentiation medium. Cidea proteins were detected on day 4 of differentiation and its levels increased upon further differentiation in wild-type but not in *Cidea*^{-/-} adipocytes (Supplementary Figure 7A). Ucp1 mRNA was also detected on day 4 and progressively increased upon further differentiation (Supplementary Figure 7B). These data indicate that MEFs differentiated under this condition acquired certain brown adipocyte characteristics and can be used as a brown adipocyte cell model. The morphology of differentiated MEFs from wild-type and *Cidea*^{-/-} mice appeared to be similar (Supplementary Figure 7C). In addition, expression

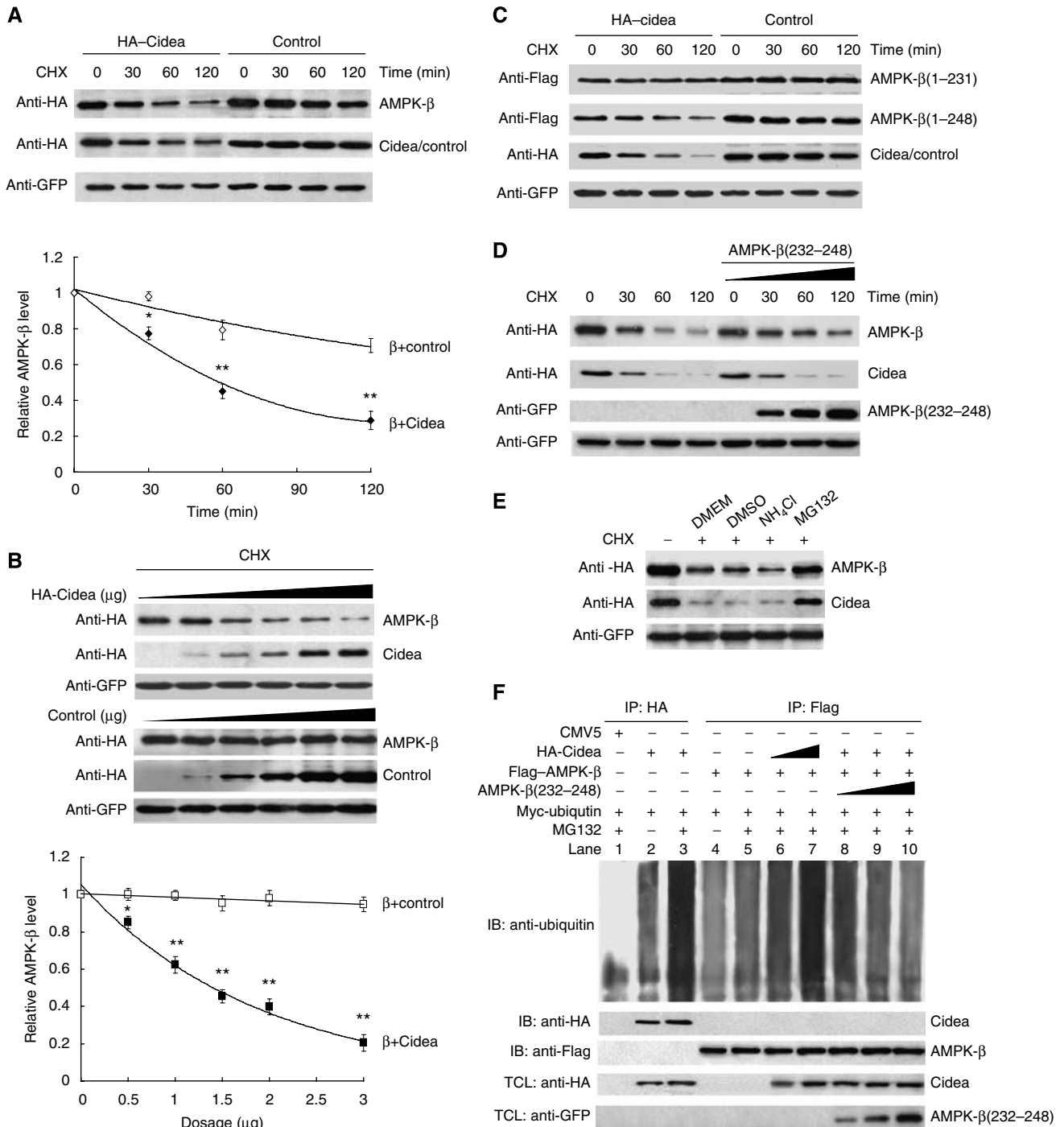


Figure 4 Cidea accelerates the degradation of AMPK- β . (A) AMPK- β protein is degraded rapidly in the presence of Cidea. HA-FADD was used as a negative control. HA-AMPK- β (1.0 μ g) was co-transfected with 1.0 μ g of HA-Cidea or HA-FADD. GFP was a transfection control. Cycloheximide (CHX) was added into the medium and cells were harvested at 0, 30, 60 and 120 min after CHX treatment. The AMPK- β level before CHX treatment was designated as 1 (* P < 0.05, ** P < 0.01). (B) Enhanced AMPK- β degradation in the presence of increasing amounts of Cidea. HA-AMPK- β was co-transfected with increasing amounts of HA-Cidea or HA-FADD. Cells were treated with CHX for 2 h before harvesting (* P < 0.05, ** P < 0.01). (C) Cidea-mediated AMPK- β degradation is dependent on their direct interaction. Flag-AMPK- β (1-231) or AMPK- β (1-248) was co-transfected with HA-Cidea or FADD (* P < 0.05, ** P < 0.01). (D) AMPK- β (232-248) attenuates Cidea-mediated AMPK- β degradation. Increasing amounts of GFP-AMPK- β (232-248) were co-transfected with HA-Cidea and HA-AMPK- β . (E) Cidea-mediated AMPK- β degradation is dependent on the proteosomal activity. MG132 (10 μ M), a proteasome-specific inhibitor; NH₄Cl (10 mM), a lysosomal protease inhibitor. DMEM containing DMSO was used as a control. (F) Cidea promotes AMPK- β ubiquitination. Myc-ubiquitin (2.0 μ g), 1.0 μ g HA-Cidea and Flag-AMPK- β were single or co-transfected. MG132 was added to a final concentration of 10 μ M for 2 h. Cidea and AMPK- β were immunoprecipitated using antibodies against HA or Flag, respectively. SDS (0.5%) was added to the immunoprecipitation buffer to disrupt the interaction between Cidea and AMPK- β . CMV5 vector was transfected as a negative control (lane 1). Cidea can be ubiquitinated and MG132 treatment resulted in higher accumulation of ubiquitinated Cidea (lanes 2 and 3, respectively); levels of AMPK- β ubiquitination in the absence or presence of MG132 (lanes 4 and 5). AMPK- β ubiquitination is enhanced in the presence of increasing amounts of Cidea (1.0 and 2.0 μ g for lanes 6 and 7, respectively). The attenuation of AMPK- β ubiquitination is seen in the presence of GFP-AMPK- β (232-248) that competes for Cidea (from 1.0 to 8.0 μ g, lanes 8-10).

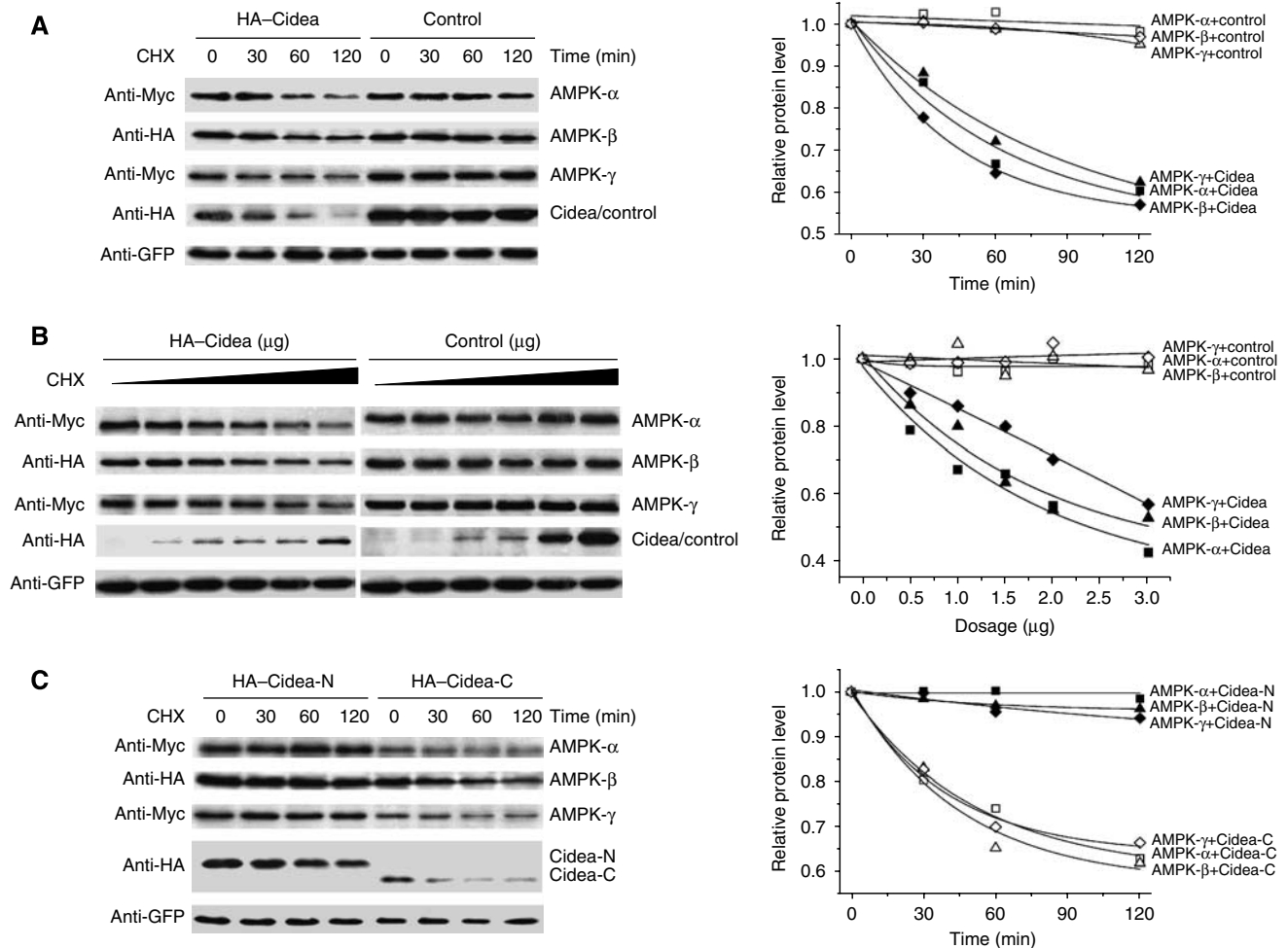


Figure 5 Cidea promotes the degradation of AMPK complex. (A) Accelerated degradation of AMPK complex when co-expressed with Cidea. Each AMPK subunit (0.1 μg) (Myc-AMPK- α , HA-AMPK- β and Myc-AMPK- γ) and 1.0 μg of HA-Cidea or HA-FADD were used for co-transfection. Statistical analysis (right panel, $P < 0.001$) was evaluated from five independent experiments. (B) Degradation of AMPK complex is dependent on the amount of Cidea. Increasing amounts of Cidea (from 0 to 2 μg) or FADD were co-transfected with AMPK complex. Experiments were repeated five times and showed significant difference ($P < 0.001$). (C) C-Terminal region of Cidea (Cidea-C) can promote AMPK complex degradation. Cidea-N or Cidea-C (1.0 μg) was co-transfected with AMPK subunits. Experiment was repeated four times and showed significant difference, $P < 0.01$.

levels of adipocyte-specific markers such as FABP and Perilipin A were similar in wild-type and *Cidea*^{-/-} adipocytes, suggesting of no defect in adipocyte differentiation in *Cidea*^{-/-} mice (Supplementary Figure 7D). We then measured protein levels of AMPK- α , - β and - γ in wild-type and *Cidea*^{-/-} adipocytes. Consistent with our observation in *Cidea*^{-/-} mice, protein levels of AMPK- α , - β and - γ were significantly increased in differentiated *Cidea*^{-/-} adipocytes (Figure 6A). AMPK activity assessed by ACC phosphorylation was also increased in *Cidea*^{-/-} adipocytes (Figure 6A), whereas total ACC levels were similar between wild-type and *Cidea*^{-/-} adipocytes. At 2 h after CHX treatment, more than 70% AMPK- β protein remained in *Cidea*^{-/-} adipocytes, whereas only 40% AMPK- β remained in wild-type adipocytes (Figure 6B; $P < 0.01$), suggesting of an increased AMPK- β stability in *Cidea*^{-/-} adipocytes. The stability of AMPK- γ was also increased in *Cidea*^{-/-} adipocytes (Figure 6B; $P < 0.05$). Increased AMPK- β and - γ stability was also observed in mature brown adipocytes differentiated from preadipocytes of BAT of *Cidea*^{-/-} mice compared with that of wild-type mice (Supplementary Figure 8A). We next checked

the level of AMPK phosphorylation and AMPK activity in wild-type and *Cidea*^{-/-} adipocytes in the presence of AICAR, an AMP analogue that stimulates AMPK activity *in vivo*. Basal and AICAR-induced AMPK- α phosphorylation and AMPK activity (levels of p-ACC) were all significantly increased in *Cidea*^{-/-} adipocytes (Figure 6C; $P < 0.05$), consistent with the increase in AMPK protein levels. Basal and AICAR-induced AMPK phosphorylation and activities were also increased in mature brown adipocytes of *Cidea*^{-/-} mice compared with that of wild-type mice (Supplementary Figure 8B). These data suggest that AMPK stability and activity are significantly increased in *Cidea*^{-/-} adipocytes differentiated either from MEFs or preadipocytes, consistent with our results from the overexpression system using other cell lines.

As AMPK promotes mitochondrial fatty acid oxidation in adipocytes, we incubated differentiated MEFs with ³H-labelled palmitic acid and observed that the rate of fatty acid oxidation in *Cidea*^{-/-} adipocytes was significantly higher than that of wild-type adipocytes at all time points tested (Figure 6D, lower panel). Although, AMPK has been reported to inhibit lipolysis in various cell types, no difference in

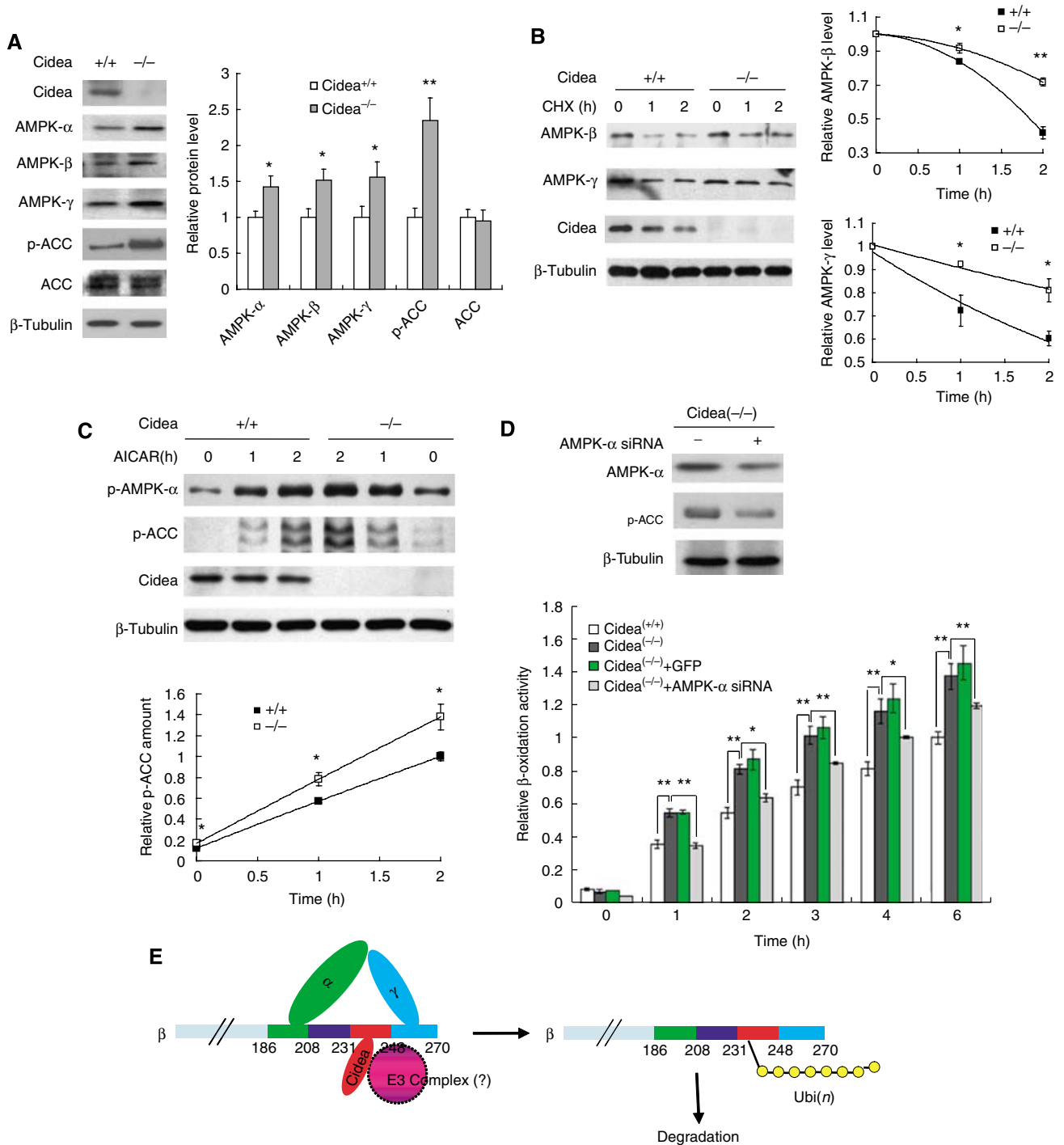


Figure 6 *Cidea*^{-/-} adipocytes showed increased AMPK protein levels, AMPK stability, activity and fatty acid oxidation rate. (A) *Cidea*^{-/-} adipocytes had increased levels of AMPK- α , - β - γ and ACC phosphorylation. MEFs isolated from wild-type and *Cidea*^{-/-} mouse embryos were induced to differentiation into a brown adipocyte like cells (M&M). Cells were collected after 8 days of differentiation and used for western blot analysis. Protein levels were normalized by β -tubulin. The right panel shows the quantitative analysis of the western blot bands. The relative protein level of each AMPK subunit, total ACC and p-ACC in wild-type adipocytes was designated as 1.0. Statistical *P*-value was calculated from three similar sets of experiments (**P* < 0.05, ***P* < 0.01). (B) Increased AMPK stability in *Cidea*^{-/-} adipocytes. MEFs 8 days after differentiation were treated with CHX (500 μ g/ml) for 1 or 2 h. The relative protein level before CHX treatment (0 hour) was designated as 1.0. **P* < 0.05. (C) Increased basal and AICAR-induced AMPK phosphorylation and activity in *Cidea*^{-/-} adipocytes. AICAR (2 mM) was added into differentiated cells for 1 or 2 h. Levels of endogenous phosphorylated AMPK- α , ACC1 and ACC2 were used to evaluate AMPK activity. The lower panel shows the quantitative analysis of the p-ACC western blot bands. Levels of p-ACC in wild-type adipocytes after 2 h of AICAR treatment was designated as 1.0. (D) *Cidea*^{-/-} adipocytes showed increased fatty acid β -oxidation, which can be attenuated by siRNA against AMPK- α . The upper panel shows the efficiency of lentiviral-mediated AMPK- α knockdown by siRNA (*Cidea*^{-/-} + AMPK- α siRNA) in *Cidea*^{-/-} adipocytes. The fatty acid β -oxidation rate of wild-type adipocytes at 6 h was designated as 1.0. The statistical results came from four replicates (**P* < 0.05, ***P* < 0.01). Lentivirus containing GFP (*Cidea*^{-/-} + GFP) was served as a negative control. (E) The proposed model for AMPK- β degradation. Ubi(*n*): polyubiquitination.

lipolysis was observed between wild-type and *Cidea*^{-/-} adipocytes (Supplementary Figure 9A). The rate of glucose uptake in differentiated MEFs was similar between wild-type and *Cidea*^{-/-} mice (Supplementary Figure 9B). Levels of phosphorylation of S6K, crucial kinase acting in the mTOR pathway, were also similar between wild-type and *Cidea*^{-/-} adipocytes (Supplementary Figure 10). Our data indicate that increased AMPK levels and enzymatic activity in brown adipocytes exert an effect primarily to enhance fatty acid oxidation. To ascertain that increased AMPK indeed is the main contributor of increased fatty acid oxidation and enhanced energy expenditure in *Cidea*^{-/-} adipocytes, we reduced the expression levels of AMPK- α by lentivirus-directed siRNA against AMPK- α . When levels of AMPK were reduced by 50% in *Cidea*^{-/-} adipocytes, β -oxidation rate was approximately 30% lower compared with that of cells infected with siRNA against GFP (Figure 6D). These data suggest that increased fatty acid β -oxidation in *Cidea*^{-/-} adipocyte is a consequence of increased levels of ACC phosphorylation and enhanced AMPK activity.

Discussion

Our previous work using *Cidea*^{-/-} mice demonstrated that mice lacking functional *Cidea* display resistance to induction of obesity through increased energy expenditure, and that *Cidea* could negatively regulate energy consumption in BAT. Here, we demonstrated that *Cidea* protein levels are increased in the BAT of HFD-fed mice and AMPK levels are inversely correlated with levels of *Cidea* in BAT. Correlation of higher protein levels of *Cidea* with obesity was also observed in mice treated with high-calorie diet (Baur *et al*, 2006). At the mRNA level, Nordstrom *et al* (2005) showed that levels of *Cidea* mRNA in the BAT of mice fed with a cafeteria diet was similar to that of animals fed with a ND; however, *Cidea* protein levels were not measured. Similar levels of mRNA could lead to different levels of protein due to post-translational regulations. We have shown that *Cidea* protein can be regulated by ubiquitin-mediated proteosomal degradation pathway (Chan *et al*, 2007). It is therefore plausible that increased *Cidea* protein in the BAT of HFD-fed animal was due to increased *Cidea* stability.

In the present study, we have further characterized the molecular changes in the *Cidea*-deficient lean mice, and have shown that the critical metabolic sensor AMPK complex is increased in its stability. Mechanistically, we have demonstrated that *Cidea* forms a complex with AMPK *in vivo* through its specific interaction with AMPK- β subunit. More importantly, by interacting with AMPK- β , *Cidea* is able to promote the heterotrimeric AMPK complex degradation, which is dependent on their physical interaction. It must be noted that when AMPK- α and - γ subunits are expressed either alone or together but without co-expression of the β subunit, their basal stability is decreased, and can no longer be further decreased by co-expression of *Cidea*. It is highly likely that when the AMPK β subunit is occupied by *Cidea* interaction, α and γ subunits may become uncomplexed and undergo rapid degradation by as yet uncharacterized mechanisms. These observations conform to the notion that *Cidea* promotes AMPK degradation by first targeting its β subunit. Furthermore, analysis of structural requirements for the *Cidea*-mediated degradation of AMPK revealed that the

C-terminal region of *Cidea* but not its N-terminal region is involved. Truncated AMPK- β proteins that lack the region (aa 232–248) required for mediating its interaction with *Cidea* no longer undergo *Cidea*-mediated protein degradation. Using specific protease inhibitors, we demonstrated that *Cidea*-induced acceleration of AMPK degradation is dependent on the ubiquitination–proteosome pathway. These data are the first to show that AMPK can be controlled by ubiquitin-dependent proteosomal degradation pathway that is mediated by its interaction with *Cidea* in the BAT. The mechanism by which *Cidea* mediates AMPK degradation is not clear. *Cidea* may help to recruit specific E3 ubiquitin ligases to AMPK- β and enhance its ubiquitination and proteosomal-dependent degradation. Alternatively, *Cidea* itself may exert an effect as an E3 ubiquitin ligase to interact with AMPK- β and enhance its ubiquitination.

Consistent with a negative regulation of *Cidea* on the stability of AMPK in the overexpression system, increased AMPK stability was seen in *Cidea*^{-/-} adipocytes differentiated from *Cidea*^{-/-} MEFs and from pre-brown adipocytes isolated from the BAT of *Cidea*^{-/-} mice. In addition, basal and AICAR-induced AMPK activities in the BAT of *Cidea*^{-/-} mice, and in the adipocytes differentiated from *Cidea*^{-/-} MEFs or pre-brown adipocytes, were all significantly increased. Interestingly, although AMPK was reported to activate multiple pathways in different cell types (Daval *et al*, 2006), lipolysis, glucose uptake or mTOR pathway were not affected in *Cidea*^{-/-} adipocytes, suggesting that additional factors are required to activate these pathways in brown adipocytes. Basal AMPK activity in BAT was reported to be high due to high levels of AMPK- α 1 expression (Mulligan *et al*, 2007). Negative regulation of AMPK by *Cidea* may help fine-tune its activity and maintain the proper balance of energy consumption under non-thermogenic condition.

We observed that majority of *Cidea* and AMPK- β proteins is localized to ER, providing a cellular basis for their molecular and functional interaction. This ER localization of *Cidea* in the BAT tissue is different from our previous observation that *Cidea*, when overexpressed in heterologous cells, were overlapped with mitochondrial marker Mitotracker (Zhou *et al*, 2003). After careful re-evaluation of the subcellular localization of *Cidea* that is ectopically expressed in many different cell types along extensive time courses, we found that the previously observed overlapping staining between *Cidea* protein and mitochondrial marker was in fact only seen at late stages during cell death when cellular structure was disrupted by *Cidea* overexpression. *Cidea* is primarily localized to the ER in most of the cells with intact morphology. Furthermore, the detection of *Cidea* protein in heavy membrane fractions of BAT (Zhou *et al*, 2003) was likely due to the contamination of ER proteins in the preparation, as endogenous *Cidea* proteins are not detected in further purified mitochondria fractions.

On the basis of our current findings, we propose a novel mechanism to explain the increased energy expenditure and lean phenotype of *Cidea*-null mice. In wild-type mice, *Cidea* interacts with AMPK- β and accelerates its degradation, resulting in reduced AMPK activity, decreased fatty acid oxidation in BAT and reduced energy expenditure. In the BAT of *Cidea*^{-/-} mice, loss of *Cidea* results in the stabilization of AMPK complex and as a result, increased AMPK protein levels as well as enhanced basal AMPK activity, which

leads to elevated fatty acid oxidation and energy expenditure in mice. The long-term effect of enhanced basal AMPK activity in the BAT will at least in part account for the lower accumulation of fat in WAT. In summary, our study has revealed a novel mechanism for AMPK regulation, in that its stability is controlled through direct interaction with Cidea, and has thus provided a possible molecular link between Cidea deficiency and the obesity-resistant phenotype seen in the *Cidea*^{-/-} mice.

Materials and methods

Materials used in this study are described in detail in Supplementary data.

Plasmid constructions

Full-length human EST clones for AMPK- α 1, - β 1 and - γ 1 were purchased from Research Genetics (USA) and subcloned into pCMV5 vectors containing HA, Flag or Myc tags. All other mutant constructs of AMPK- β 1 and Cidea were created by PCR-based mutagenesis and verified by DNA sequencing. Primer information for all constructs will be available upon request. AMPK- α siRNA was designed according to the previous report (Cidad *et al*, 2004), constructed into FG12 expression vector (generous gift from Dr Zilong Wen, HKUST) and packaged into lentivirus as previously described (Dull *et al*, 1998).

Mice handling, cell culture and transfection, co-immunoprecipitation, and western blot analysis, immunofluorescent staining

Procedures for mouse handling, cell culture and transfection, co-immunoprecipitation, immunofluorescent staining and western blot analysis were essentially the same as described previously (Zhou *et al*, 2003) and in Supplementary data. MEFs were isolated from embryonic day 12.5 wild-type and *Cidea*^{-/-} mouse embryos (Phan *et al*, 2004). MEFs were differentiated into brown adipocytes in the differentiation medium containing 10% FBS, 8 μ g/ml D-pantothenic acid, 8 μ g/ml biotin, 0.5 μ M triiodothyronine (T3), 1 μ M dexamethasone, 0.5 mM 3-isobutyl-1-methylxanthine, 5 μ g/ml insulin, 1 μ M pioglitazone (Beijing Taiyang Pharmaceutical Industry Co.).

Biochemical fractionation of subcellular organelles in BAT and gel filtration analysis

Procedures for isolation of subcellular organelles were essentially the same as described (Croze and Morre, 1984) with minor modification (Supplementary data). Cytosolic fraction was concentrated with PEG 8000 to final volume of 500 μ l. Fractions for Golgi, ER, mitochondrial and nuclei were resuspended with 50 μ l of protein loading buffer and used for western blot analysis. Cytosolic fraction was analysed on a Superdex 200 10/300 GL column (FPLC; Pharmacia, USA) with a flow rate of 0.4 ml/min. Fractions were frozen dried and dissolved in 40 μ l 10 mM Tris-HCl (pH 8.0) for western blot analysis.

References

- Baba M, Hong SB, Sharma N, Warren MB, Nickerson ML, Iwamatsu A, Esposito D, Gillette WK, Hopkins III RF, Hartley JL, Furihata M, Oishi S, Zhen W, Burke Jr TR, Linehan WM, Schmidt LS, Zbar B (2006) Folliculin encoded by the BHD gene interacts with a binding protein, FNIP1, and AMPK, and is involved in AMPK and mTOR signaling. *Proc Natl Acad Sci USA* **103**: 15552–15557
- Banerjee RR, Rangwala SM, Shapiro JS, Rich AS, Rhoades B, Qi Y, Wang J, Rajala MW, Poci A, Scherer PE, Stepan CM, Ahima RS, Obici S, Rossetti L, Lazar MA (2004) Regulation of fasted blood glucose by resistin. *Science* **303**: 1195–1198
- Baur JA, Pearson KJ, Price NL, Jamieson HA, Lerin C, Kalra A, Prabhu VV, Allard JS, Lopez-Lluch G, Lewis K, Pistell PJ, Poosala S, Becker KG, Boss O, Gwinn D, Wang M, Ramaswamy S, Fishbein KW, Spencer RG, Lakatta EG *et al* (2006) Resveratrol improves health and survival of mice on a high-calorie diet. *Nature* **444**: 337–342

AMPK kinase activity assay

Protocols for AMPK kinase assay were modified from previous report (Davies *et al*, 1989) and described in detail in Supplementary data. For measuring AMPK activity in BAT, total BAT lysates were subjected to protein precipitation by 2.5–6% (w/v) of PEG 8000 (Kudo *et al*, 1995), and 5 μ g of such prepared proteins was used for each assay reaction. To measure endogenous AMPK activity, MEFs were differentiated for 8 days and then incubated with or without 2 mM AICAR (Sakoda *et al*, 2002) for various durations.

AMPK stability assay

AMPK stability was measured by CHX-based protein-chase experiment. Details for such experiment were described in Supplementary data. Expression plasmids in various combinations were transfected into 293T cells by the calcium phosphate method. At 24 h post-transfection, the medium was replaced with fresh DMEM plus 10% FBS followed by addition of CHX (100 μ g/ml) 1 h later. Cells were harvested at four different time points (0, 30, 60 and 120 min) after the addition of CHX, and were lysed in a 0.5-ml lysis buffer. Levels of AMPK subunits were analysed by western blotting analysis. To measure endogenous AMPK stability, a final concentration of 500 μ g/ml CHX was added into 8-day differentiated adipocytes.

ACC enzymatic activity and fatty acid oxidation

Acetyl-CoA carboxylase activity was determined using the [¹⁴C]bicarbonate fixation assay (Majerus *et al*, 1968). Fatty acid oxidation measurement procedure was essentially the same as described by Moon and Rhead (1987) using [9,10(*n*)-³H]palmitic acid (1.0 μ Ci per well; Amersham) with 22 μ M unlabelled palmitic acid and 0.5 mg/ml fatty acid-free BSA in the reaction. The radioactivity in aqueous phase containing ³H₂O was collected and used for radioactivity measurement. Details of the procedures are described in Supplementary data.

Supplementary data

Supplementary data are available at *The EMBO Journal* Online (<http://www.embojournal.org>).

Acknowledgements

We thank members in Peng Li's Laboratory in Tsinghua University and HKUST for technical assistance and helpful discussion. We also thank Dr SC Lin for critical editing of the paper. This study was supported by grants (HKUST6233/03 to PL) from Hong Kong Research Grant Council; (30429001 and 30530350 to PL) from National Natural Science Foundation of China; (704002 to PL) from Ministry of Education of China; and National Basic Research program of China (2006CB503900, 2007CB914404) from Ministry of Science and Technology of China. We are grateful to the technical help provided by Miss Luxin Yu and Mr Shuqun Yang in Tsinghua University. This study was also supported by Program for Changjiang Scholars and Innovative Research Team in University from Ministry of Education in China.

- Chan SC, Lin SC, Li P (2007) Regulation of Cidea protein stability by the ubiquitin-mediated proteasomal degradation pathway. *Biochem J* **408**: 259–266
- Chen Z, Guo K, Toh SY, Zhou Z, Li P (2000) Mitochondria localization and dimerization are required for CIDE-B to induce apoptosis. *J Biol Chem* **275**: 22619–22622
- Cidad P, Almeida A, Bolanos JP (2004) Inhibition of mitochondrial respiration by nitric oxide rapidly stimulates cytoprotective GLUT3-mediated glucose uptake through 5'-AMP-activated protein kinase. *Biochem J* **384**: 629–636
- Croze EM, Morre DJ (1984) Isolation of plasma membrane, Golgi apparatus, and endoplasmic reticulum fractions from single homogenates of mouse liver. *J Cell Physiol* **119**: 46–57
- Crute BE, Seefeld K, Gamble J, Kemp BE, Witters LA (1998) Functional domains of the alpha1 catalytic subunit of the AMP-activated protein kinase. *J Biol Chem* **273**: 35347–35354

- Dahlman I, Kaaman M, Jiao H, Kere J, Laakso M, Arner P (2005) The CIDEA gene V115F polymorphism is associated with obesity in Swedish subjects. *Diabetes* **54**: 3032–3034
- Daval M, Diot-Dupuy F, Bazin R, Hainault I, Viollet B, Vaulont S, Hajdouch E, Ferre P, Foufelle F (2005) Anti-lipolytic action of AMP-activated protein kinase in rodent adipocytes. *J Biol Chem* **280**: 25250–25257
- Daval M, Foufelle F, Ferre P (2006) Functions of AMP-activated protein kinase in adipose tissue. *J Physiol* **574**: 55–62
- Davies SP, Carling D, Hardie DG (1989) Tissue distribution of the AMP-activated protein kinase, and lack of activation by cyclic-AMP-dependent protein kinase, studied using a specific and sensitive peptide assay. *Eur J Biochem* **186**: 123–128
- Dobrzyn P, Dobrzyn A, Miyazaki M, Cohen P, Asilmaz E, Hardie DG, Friedman JM, Ntambi JM (2004) Stearoyl-CoA desaturase 1 deficiency increases fatty acid oxidation by activating AMP-activated protein kinase in liver. *Proc Natl Acad Sci USA* **101**: 6409–6414
- Dull T, Zufferey R, Kelly M, Mandel RJ, Nguyen M, Trono D, Naldini L (1998) A third-generation lentivirus vector with a conditional packaging system. *J Virol* **72**: 8463–8471
- Gummesson A, Jernas M, Svensson PA, Larsson I, Glad CA, Schele E, Gripeteg L, Sjöholm K, Lystig TC, Sjöström L, Carlsson B, Fagerberg B, Carlsson LM (2007) Relations of adipose tissue cell death-inducing DFFA-like effector A gene expression to basal metabolic rate, energy restriction and obesity: population-based and dietary intervention studies. *J Clin Endocrinol Metab* **92**: 4739–4765
- Hallows KR, Raghuram V, Kemp BE, Witters LA, Foskett JK (2000) Inhibition of cystic fibrosis transmembrane conductance regulator by novel interaction with the metabolic sensor AMP-activated protein kinase. *J Clin Invest* **105**: 1711–1721
- Hardie DG, Hawley SA, Scott JW (2006) AMP-activated protein kinase—development of the energy sensor concept. *J Physiol* **574**: 7–15
- Hawley SA, Boudeau J, Reid JL, Mustard KJ, Udd L, Makela TP, Alessi DR, Hardie DG (2003) Complexes between the LKB1 tumor suppressor, STRAD alpha/beta and MO25 alpha/beta are upstream kinases in the AMP-activated protein kinase cascade. *J Biol* **2**: 28
- Hawley SA, Pan DA, Mustard KJ, Ross L, Bain J, Edelman AM, Frenguelli BG, Hardie DG (2005) Calmodulin-dependent protein kinase kinase-beta is an alternative upstream kinase for AMP-activated protein kinase. *Cell Metab* **2**: 9–19
- Hurley RL, Anderson KA, Franzone JM, Kemp BE, Means AR, Witters LA (2005) The Ca²⁺/calmodulin-dependent protein kinase kinases are AMP-activated protein kinase kinases. *J Biol Chem* **280**: 29060–29066
- Huypens P, Quartier E, Pipeleers D, Van de Casteele M (2005) Metformin reduces adiponectin protein expression and release in 3T3-L1 adipocytes involving activation of AMP-activated protein kinase. *Eur J Pharmacol* **518**: 90–95
- Inohara N, Koseki T, Chen S, Wu X, Nunez G (1998) CIDE, a novel family of cell death activators with homology to the 45 kDa subunit of the DNA fragmentation factor. *EMBO J* **17**: 2526–2533
- Inoki K, Zhu T, Guan KL (2003) TSC2 mediates cellular energy response to control cell growth and survival. *Cell* **115**: 577–590
- Iseli TJ, Walter M, van Denderen BJ, Katsis F, Witters LA, Kemp BE, Michell BJ, Stapleton D (2005) AMP-activated protein kinase beta subunit tethers alpha and gamma subunits via its C-terminal sequence (186–270). *J Biol Chem* **280**: 13395–13400
- Kahn BB, Alquier T, Carling D, Hardie DG (2005) AMP-activated protein kinase: ancient energy gauge provides clues to modern understanding of metabolism. *Cell Metab* **1**: 15–25
- Kishi K, Yuasa T, Minami A, Yamada M, Hagi A, Hayashi H, Kemp BE, Witters LA, Ebina Y (2000) AMP-Activated protein kinase is activated by the stimulations of G(q)-coupled receptors. *Biochem Biophys Res Commun* **276**: 16–22
- Kudo N, Barr AJ, Barr RL, Desai S, Lopaschuk GD (1995) High rates of fatty acid oxidation during reperfusion of ischemic hearts are associated with a decrease in malonyl-CoA levels due to an increase in 5'-AMP-activated protein kinase inhibition of acetyl-CoA carboxylase. *J Biol Chem* **270**: 17513–17520
- Lee JH, Koh H, Kim M, Kim Y, Lee SY, Karess RE, Lee SH, Shong M, Kim JM, Kim J, Chung J (2007) Energy-dependent regulation of cell structure by AMP-activated protein kinase. *Nature* **447**: 1017–1020
- Long YC, Zierath JR (2006) AMP-activated protein kinase signaling in metabolic regulation. *J Clin Invest* **116**: 1776–1783
- Majerus PW, Jacobs R, Smith MB, Morris HP (1968) The regulation of fatty acid biosynthesis in rat hepatomas. *J Biol Chem* **243**: 3588–3595
- Minokoshi Y, Kim YB, Peroni OD, Fryer LG, Muller C, Carling D, Kahn BB (2002) Leptin stimulates fatty-acid oxidation by activating AMP-activated protein kinase. *Nature* **415**: 339–343
- Moon A, Rhead WJ (1987) Complementation analysis of fatty acid oxidation disorders. *J Clin Invest* **79**: 59–64
- Mulligan JD, Gonzalez AA, Stewart AM, Carey HV, Saupé KW (2007) Upregulation of AMPK during cold exposure occurs via distinct mechanisms in brown and white adipose tissue of the mouse. *J Physiol* **580**: 677–684
- Nordstrom EA, Ryden M, Backlund EC, Dahlman I, Kaaman M, Blomqvist L, Cannon B, Nedergaard J, Arner P (2005) A human-specific role of cell death-inducing DFFA (DNA fragmentation factor-alpha)-like effector A (CIDEA) in adipocyte lipolysis and obesity. *Diabetes* **54**: 1726–1734
- Phan J, Peterfy M, Reue K (2004) Lipin expression preceding peroxisome proliferator-activated receptor-gamma is critical for adipogenesis *in vivo* and *in vitro*. *J Biol Chem* **279**: 29558–29564
- Ross SR, Choy L, Graves RA, Fox N, Solevjeva V, Klaus S, Ricquier D, Spiegelman BM (1992) Hibernoma formation in transgenic mice and isolation of a brown adipocyte cell line expressing the uncoupling protein gene. *Proc Natl Acad Sci USA* **89**: 7561–7565
- Sakoda H, Ogihara T, Anai M, Fujishiro M, Ono H, Onishi Y, Katagiri H, Abe M, Fukushima Y, Shojima N, Inukai K, Kikuchi M, Oka Y, Asano T (2002) Activation of AMPK is essential for AICAR-induced glucose uptake by skeletal muscle but not adipocytes. *Am J Physiol Endocrinol Metab* **282**: E1239–E1244
- Salt I, Celler JW, Hawley SA, Prescott A, Woods A, Carling D, Hardie DG (1998) AMP-activated protein kinase: greater AMP dependence, and preferential nuclear localization, of complexes containing the alpha2 isoform. *Biochem J* **334** (Part 1): 177–187
- Scott JW, Hawley SA, Green KA, Anis M, Stewart G, Scullion GA, Norman DG, Hardie DG (2004) CBS domains form energy-sensing modules whose binding of adenosine ligands is disrupted by disease mutations. *J Clin Invest* **113**: 274–284
- Spiegelman BM, Flier JS (2001) Obesity and the regulation of energy balance. *Cell* **104**: 531–543
- Steinberg GR, Macaulay SL, Febbraio MA, Kemp BE (2006) AMP-activated protein kinase—the fat controller of the energy railroad. *Can J Physiol Pharmacol* **84**: 655–665
- Townley R, Shapiro L (2007) Crystal structures of the adenylate sensor from fission yeast AMP-activated protein kinase. *Science* **315**: 1726–1729
- Warden SM, Richardson C, O'Donnell Jr J, Stapleton D, Kemp BE, Witters LA (2001) Post-translational modifications of the beta-1 subunit of AMP-activated protein kinase affect enzyme activity and cellular localization. *Biochem J* **354**: 275–283
- Woods A, Dickerson K, Heath R, Hong SP, Momcilovic M, Johnstone SR, Carlson M, Carling D (2005) Ca²⁺/calmodulin-dependent protein kinase kinase-beta acts upstream of AMP-activated protein kinase in mammalian cells. *Cell Metab* **2**: 21–33
- Woods A, Johnstone SR, Dickerson K, Leiper FC, Fryer LG, Neumann D, Schlattner U, Wallimann T, Carlson M, Carling D (2003) LKB1 is the upstream kinase in the AMP-activated protein kinase cascade. *Curr Biol* **13**: 2004–2008
- Xiao B, Heath R, Saiu P, Leiper FC, Leone P, Jing C, Walker PA, Haire L, Eccleston JF, Davis CT, Martin SR, Carling D, Gamblin SJ (2007) Structural basis for AMP binding to mammalian AMP-activated protein kinase. *Nature* **449**: 496–500
- Xue B, Kahn BB (2006) AMPK integrates nutrient and hormonal signals to regulate food intake and energy balance through effects in the hypothalamus and peripheral tissues. *J Physiol* **574**: 73–83
- Yamauchi T, Kamon J, Minokoshi Y, Ito Y, Waki H, Uchida S, Yamashita S, Noda M, Kita S, Ueki K, Eto K, Akanuma Y, Froguel P, Foufelle F, Ferre P, Carling D, Kimura S, Nagai R, Kahn BB, Kadowaki T (2002) Adiponectin stimulates glucose utilization and fatty-acid oxidation by activating AMP-activated protein kinase. *Nat Med* **8**: 1288–1295
- Zhou Z, Yon Toh S, Chen Z, Guo K, Ng CP, Ponniah S, Lin SC, Hong W, Li P (2003) Cidea-deficient mice have lean phenotype and are resistant to obesity. *Nat Genet* **35**: 49–56